applied sciences

MDPI

Article

Removal of Nitrogen and Phosphorus in Synthetic Stormwater Runoff by a Porous Asphalt Pavement System with Modified Zeolite Powder Porous Microsphere as a Filter Column

Hui Luo [1,2], Baojie He [3,4], Wenhao Zhang [2] and Zhaoqian Jing [1,*]

1 College of Civil Engineering, Nanjing Forestry University, Nanjing 210037, China; water@njfu.edu.cn
2 College of Civil and Ocean Engineering, Jiangsu Ocean University, Lianyungang 222005, China; whzhang668@126.com
3 Centre for Climate-Resilient and Low-Carbon Cities, School of Architecture and Urban Planning, Chongqing University, Chongqing 400045, China; baojie.he@cqu.edu.cn
4 Key Laboratory of New Technology for Construction of Cities in Mountain Area, Ministry of Education, Chongqing University, Chongqing 400045, China
* Correspondence: zqjing@njfu.edu.cn; Tel.: +86-139-1596-7569

Abstract: Porous asphalt pavement (PAP) system is a widely used treatment measure in sustainable stormwater management and groundwater recharge, but their variable performance in nitrogen (N) and phosphorus (P) removal requires further reinforcement prior to widespread uptake. Two laboratory-scale PAP systems were developed by comparing limestone bedding and zeolite incorporated into modified zeolite powder porous microsphere (MZP-PM) as a filter column under a typical rainfall. The PAP system of zeolite bedding incorporated into MZP-PM (a weight less than 5% of zeolite) removed 74.5% to 90.6% of ammonium (NH_4^+-N) and 72.9% to 92.4% of total phosphate (TP) from the influent, as compared with 25.7% to 62.7% of NH_4^+-N and 32.6% to 56.4% of TP by that of the limestone as bed material. This improvement was presumably due to MZP-PM's high adsorption capacity and surface complexation. The formation of $\equiv$(La)(OH)PO_2 was verified to be the dominant pathway for selective phosphate adsorption by MZP-PM and ion-exchange was proved to be the main removal process for ammonium. This study provides promising results for improving N and P removal by modifying a porous asphalt pavement system to include an MZP-PM adsorbent column as a post-treatment.

Keywords: nutrients removal; porous asphalt pavement system; modified zeolite powder porous microspheres; ion exchange; Nemerow pollution index

check for updates

Citation: Luo, H.; He, B.; Zhang, W.; Jing, Z. Removal of Nitrogen and Phosphorus in Synthetic Stormwater Runoff by a Porous Asphalt Pavement System with Modified Zeolite Powder Porous Microsphere as a Filter Column. *Appl. Sci.* **2021**, *11*, 10810. https://doi.org/10.3390/app112210810

Academic Editor: Jorge Rodríguez-Chueca

Received: 13 October 2021
Accepted: 11 November 2021
Published: 16 November 2021

1. Introduction

A series of biochemical and physical changes occurred in the urban environment due to rapid urbanization, including a considerable increase in the stormwater runoff volume and water receiving bodies degradation [1]. The porous asphalt pavement (PAP) system can potentially minimize the influence of stormwater runoff in the ecology, hydrology, and quality of water receiving bodies simultaneously, which has been implemented worldwide [2]. As reported, the PAP system exhibits high removal capacity for various heavy metals [3], suspended solids [4], and oils [5], while the removal efficiency of nutrients such as phosphorus (P) [6] and nitrogen (N) [7] are unsatisfactory.

The quality of water is closely associated with N and P, and excessive N and P would lead to eutrophication [8]. As quantities of N and P in urban environments result from stormwater runoff, effective measurements are needed to control before draining [9]. N removal by porous asphalt pavement varied significantly, which is overall ineffective in an extended period, mainly due to the limited capacity of adsorption and short contact time of bituminous mixtures and gravel [10]. Nonetheless, studies also showed that the PAP system may remove pollutants by biological degradation [11], adsorption [12], and

export of nitrate under suitable conditions through nitrification in the sub-base. As a result, researchers are devoted to increasing the ammonia nitrogen (NH_4^+-N) adsorption [6] by various new materials under a saturated zone to improve the elimination of NH_4^+-N [13], but the saturated zone affects the removing performance of the N by high variability, which influences the strength and stability of the PAP system [7]. Consequently, the improvement in the removal of total nitrogen (TN) is negligible due to nitrate denitrification in the presence of a saturated zone [14]. The total phosphorus (TP) contained dissolved phosphorus (DP) and particulate phosphorus (PP) which were transported by stormwater runoff. The PAP system has a high efficiency of removing PP, however, it is less effective in removing DP because its removal mainly depends on P chemisorptions [6]. Razzaghmanesh et al. reported that the P removal in the PAP system mainly relied on the absorption of voids into the asphalt mixture and the precipitation on the surface of gravel and the adsorption ability of the materials in the PAP system for P were affected significantly by the content of calcium carbonate. Moreover, materials with abundant compounds of calcium and lanthanum probably influence the removal of P from wastewater [15]. Lanthanum-modified adsorbents particularly demonstrate several promising advantages during phosphate removal such as their superior adsorption capacity, wide operating pH range, and high removal rate (96%) at low phosphate concentrations. Thus, the P removal may be enhanced by integrating such compounds into the media applied in the PAP system. Zeolite has been broadly explored for the removal of ammonium due to its high capacity of cationic exchange, which has been affirmed as a promising material for its removal from contaminated waters. In addition, the adsorption capacity of the modified zeolite for nitrogen and phosphorus was significantly improved [16]. It was easy to form powder under the impact of heavy rainfall because of the fine zeolite particles. These defects limited the application of zeolite in stormwater runoff treatment. In view of such problems, the development of an adsorbent with high adsorption capacity utilized in the PAP system to remove N and P simultaneously with shallower depths and smaller space would be a way worth considering.

NaOH-activated with $LaCl_3$-impregnated synthetic modified zeolite porous microspheres (MZP-PM) were designed in this research. Negatively charged zeolite could act as good adsorbents to remove cationic pollutants from water [17]. Through the modification of zeolites, MZP-PM was produced by the method of surface activation at high-temperature roasting after adding adhesive and porous former, which was applied as a filter column in the PAP system. This research developed a novel MZP-PM and zeolite bed in the PAP system for the first time to remove nitrogen and phosphorus in stormwater runoff.

The addition of MZP-PM as a filter column and bedding layer in a PAP system was expected to enhance the elimination of P and N, both from the runoff of stormwater by four main ways. Firstly, a significant increase was caused in water retention by bedding materials [18], promoting the contact time. Secondly, alkaline and lanthanum amendment could enhance N and P removal by exchanging with sodium for NH_4^+-N and surface complexion for TP [16]. Thirdly, the increase in the particular surface area of MZP-PM gives a large number of adsorption sites during stormwater infiltration, resulting in remarkable improvement in the adsorption capacity [15]. Moreover, MZP-PM exhibits a highly stable performance, which enables the PAP system to remove nutrients without the external output of zeolite powder.

In this research, a novel technology to improve water quality in the PAP system was proposed by the post-treatment of a filter column containing MZP-PM. The influences of water quality on the two laboratory-scale PAP systems were evaluated by comparing limestone bedding and natural zeolite incorporated into MZP-PM as a filter column under a typical rainfall. The forms of ammonium and phosphate are identified onto the loaded MZP-PM, meanwhile, the mechanism of ammonium and phosphate removals are studied. Findings from the laboratory experiments were employed in optimizing the removal of nutrients from stormwater runoff by the PAP system.

2. Materials and Methods

2.1. Materials

In the PAP system, limestone and zeolite were used as bedding material. Zeolite was a kind of locally available material with the characteristics of low cost and good adsorption capacity to phosphate [16,19]. The material adopted in the experiment was obtained from a natural deposit site at Xinyang, Henan, China. The adsorbent was prepared by the improved method of sinter synthesis as follows: Firstly, 10.0 g of zeolite powder (200 mesh) was mixed at the stirring rate of 200 rpm for 8 h into a 500 mL beaker containing 200 mL of 1 M NaOH aqueous solution, then the modified zeolite powder was dried at 373 k for 6 h. Secondly, NaOH-activated zeolite was added into a 0.8% solution of $LaCl_3$ with a pH of 10.0 at the agitation of 180 rpm for 6 h. This process supported the incorporation of La on the activated zeolite surface. The acquired material was rinsed with distilled water and dried at 373 K for 12 h. Finally, the modified zeolite powder was mixed with the pore-forming agent particles (walnut sand) and the binder (sodium silicate) in a certain ratio, and a suitable amount of water was added into the pore making machine to make microspheres of 2 mm. After drying for a while, it was calcinated at 500 °C, Figure 1 shows the details of the preparation of modified zeolite powder porous microsphere used in the experiment.

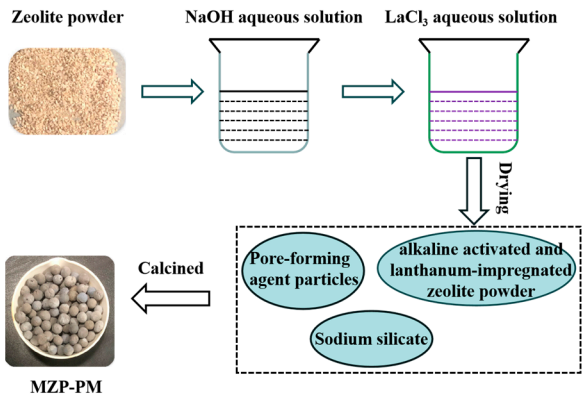

Figure 1. Preparation of modified zeolite powder porous microsphere.

2.2. Experimental Setup

Two PAP systems were assembled parallel with the dimensions of 0.3 m × 0.3 m × 0.7 m (length × width × height) in perspex containers (Figure 2). Each perspex container was packed with 10 cm porous asphalt concrete (PAC) with a void ratio of 24.2%, and 30 cm crushed gravel with a void ratio of 37.6%. Below the gravel, in one PAP system a normal size limestone bedding layer of 1–2 mm was set with a height of 20 mm and in the second PAP system, a zeolite bedding layer was placed with the same dimensions. Both PAP systems have the same volume in each layer to make them identical in dimensions. To separate the surface layer and the choker course a permeable non-woven geotextile membrane was set at the upper level [20].

The outlet of the zeolite-based PAP system was joined to a horizontal filter column (50 mm × 600 mm × 50 mm) packed with modified zeolite powder porous microspheres (MZP-PM) to enhance nitrogen and phosphorus removal. The horizontal filter column was packed with 1.2 kg material into a 600-mm long polyvinyl chloride (PVC) column. To drain water from the column's outlet, a peristaltic pump was connected.

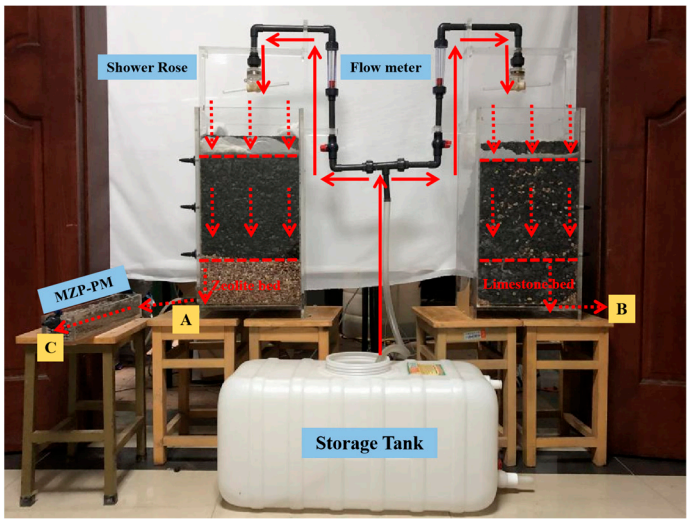

Figure 2. Porous asphalt pavement bedding and sub-base arrangement used in the laboratory experiment.

Throughout the experiments to ensure a constant quality of water, synthetic runoff stormwater was prepared by mixing de-chlorinated tap water with sediments collected from a local stormwater wetland with different concentrations of nitrogen and phosphorus (NH_4^+-N and TP). The concentrations of NH_4^+-N were 5.2 ± 0.2 mg/L and TP were 1.2 ± 0.1 mg/L, the same as reported by the urban stormwater runoff [21,22]. A simulated event of rainfall with total precipitation (82.31 mm), an average intensity (0.63 mm/min), rainfall duration (120 min), and 5 years return period were designed through the Rainstorm Intensity Formula of Nanjing. While the renowned Chicago method [23] was adopted to design the temporal distribution of the event, the rainfall event with 120 min of duration, step time of 5 min, 5 years of return period and γ = 0.40 were set as in the experiment. Samples were collected from the initial flushing effluent to evaluate the preliminary effects of the PAP approach on the removal of NH_4^+-N and TP, and the sample was collected every 15 min from the time of water discharge in the study.

2.3. Batch Experiments

Laboratory batch experiments were conducted to understand the nutrients' removal efficiencies of the basalt bed, zeolite bed and MZP-PM filter. Batch experiment data was used to obtain batch adsorption isotherm of these materials. Adsorption tests were performed at the initial concentration of N and P of 20 mg/L and 5 mg/L, respectively, and shaken with different doses of zeolite, basalt or MZP-PM in 100 mL solutions. The suspensions were agitated at 180 rpm for 12 h at 25 ± 0.5 °C and pH 6.5. The amount of nutrients adsorption at equilibrium, q_e (mg/g) was calculated using Equation (1):

$$q_e = \frac{(C_0 - C_e)V}{M} \quad (1)$$

where, C_0 is the initial concentration of NH_4^+-N and TP (mg/L), C_e is the equilibrium concentration of NH_4^+-N and TP (mg/L), V is the volume of solution (L), and M is mass of adsorbent (g).

2.4. Analytical and Characterization Methods

Ammonium and phosphate concentration were measured by Nessler's reagent colorimetric method (limit of quantification 0.025 mg/L) and the ammonium molydate spectrophotometric methods (limit of quantification 0.01 mg/L) with the spectrophotometer at 420 nm and 700 nm (UV-2550, Shimadzu, Japan), respectively. The concentration of metal ions (Na^+, K^+, Ca^{2+}, Mg^{2+}) was determined by means of atomic absorption spectrophotometry (AAS, Aoyan, China). Surface morphology and chemical compositions

of the absorbent were determined by scanning electron microscopy (SEM, ZEISS-EVO18, Germany) and energy-dispersive X-ray spectroscopy (EDS, INCA ENERGY 350, UK). FTIR spectra were collected on Nicolet IS10 FTIR spectrophotometer (Bruker -Alpha, V70, Thermo scientific, New York, NY, USA) using a transmission model from 400 to 4000 cm^{-1}. X-ray photoelectron spectra (XPS) were collected on Kratos Axis Ultra DLD instrument equipped with a mono-chromated Al Kα irradiation. The XPS results were collected in binding energy forms and fitted using a nonlinear least-squares curve-fitting program (XPSPEAK41 Software. Versions: 4.1).

2.5. Assessment of Water Quantity

The extent of pollutant concentrations was assessed by comparing water quality parameters against a range of national criteria. The pollutant indicators NH_4^+-N and TP were assessed for compliance with Class IV of Surface Water Environmental Quality Standards of China (GB3838-2002) and Class I-B of Discharge Standard of Pollutants for Municipal Wastewater Treatment Plant of China (GB18918-2002).

Nemerow Index Method is commonly used to evaluate the integrated and comprehensive pollution status of the pollutants of a water body. In this method, a single factor index was firstly calculated, then the average values were determined and finally, the maximum value was selected and used to calculate the Nemerow index value, as per the following formula [24,25]; The calculation formulas are as followed:

$$P_i = \frac{C_i}{S_i} \tag{2}$$

$$\overline{P_i} = \frac{1}{n}\sum_{1}^{n}\frac{C_i}{S_i} \tag{3}$$

$$P_{i\ max} = \max\left\{\frac{C_i}{S_i}\right\} \tag{4}$$

$$P_n = \sqrt{\frac{P_{i\ max}^2 + \overline{P_i^2}}{2}} \tag{5}$$

where P_i is the single factor index of individual pollutants, C_i represents the actual measured concentration of pollutants in the effluent and S_i represents the standard guideline concentration of the respective pollutants (based on water quality standards of Grade V for surface water in China). P_n represents the integrated index, the Nemerow index which explains the extent of nutrient pollution, $\overline{P_i}$ indicates the mean value of and P_{imax} represents the maximum value of P_i. This method will provide a rational interpretation of nutrient contamination at each sampling time as a whole.

3. Results

3.1. Batch Experiments

The batch adsorption data (Figure 3) were analyzed through the Langmuir and Freundlich adsorption models [26]. The corresponding model constants and correlation coefficients are summarized in Table 1. The Langmuir adsorption model fitted well to the data for the nutrients in all three materials (R^2 = 0.962–0.997), demonstrating that the adsorption sites on these materials were homogeneous with monolayer adsorption coverage. The Freundlich model fitted satisfactorily to the data only for zeolite and limestone bedding materials. However, the model fitting to the data was generally better through the Langmuir model compared with that using the Freundlich model, especially for basalt bedding material and MZP-PM. The deviation of NH_4^+-N adsorption data for MZP-PM was relatively large upon fitting through the Freundlich model, which agrees well with previously reported results when using modified zeolite adsorbent [19,27].

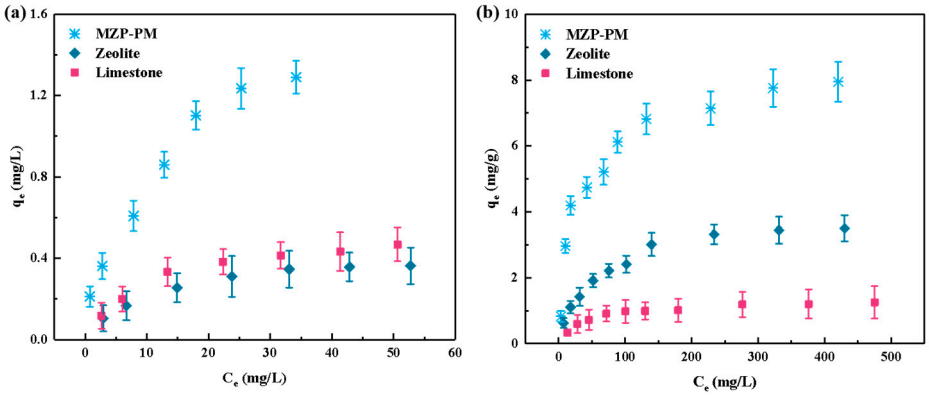

Figure 3. Adsorption isotherms of NH_4^+-N (**a**) and TP (**b**) at pH 6.5 for zeolite, limestone and MZP-PM. (C_e is the equilibrium concentration of pollutants, mg/L; q_e is the adsorption capacity at equilibrium, mg/g).

Table 1. Langmuir and Freundlich model parameters for NH_4^+-N and TP adsorption in zeolite, limestone and MZP-PM, and coefficients of determination for the models fits the data (R^2).

Material	Pollutants	Langmuir			Freundlich		
		Q_{max} (mg/g)	R^2	K_L (L/mg)	K_F (mg/g (L/mg)$^{1/n}$	1/n	R^2
Limestone	NH_4^+-N	1.31	0.992	0.053	0.11	0.71	0.917
	TP	0.55	0.997	0.103	0.17	0.59	0.981
Zeolite	NH_4^+-N	3.34	0.986	0.036	0.32	0.43	0.956
	TP	0.42	0.994	0.112	0.14	0.63	0.954
MZP-PM	NH_4^+-N	9.72	0.972	0.028	0.91	0.39	0.923
	TP	1.23	0.965	0.32	0.23	0.49	0.946

K_L and K_F are the correlation constants of Langmuir and Freundlich models respectively, n is an empirical constant reflecting the adsorption capability, R^2 is the correlation coefficient in the fitting process.

The maximum of Langmuir adsorption was obtained from the linear plot slope of the Ce/Qe vs. Ce for the pollutants followed the order of NH_4^+-N > TP for all of the bedding materials. The order of adsorption capacities of the three bedding materials were MZP-PM > zeolite > limestone for NH_4^+-N and MZP-PM > limestone > zeolite for TP. This result demonstrates that the MZP-PM was the best among the three kinds of materials. The maximum adsorbed capacities by Langmuir adsorption model were 9.72 mg/g and 1.23 mg/g for NH_4^+-N and TP, respectively; for MZP-PM, exhibiting the enhancement of 7.4 and 1.7 times by limestone (1.31 mg/g for NH_4^+-N and 0.55 mg/g for TP) respectively, which was superior to other adsorption systems in dealing with stormwater runoff [28]. Previous studies also showed the lanthanum-modified bentonite adsorbent [29] had greater phosphate adsorption capacity than MZP-PM, while nitrogen and phosphate could not be removed simultaneously. Thus, it probably provides the potential to be a capable adsorbent in the PAP system to stormwater for NH_4^+-N and TP removal.

3.2. Removal of Ammonium and Phosphate in PAP Systems

The removal efficiency during a typical rainfall for NH_4^+-N and TP was shown in Figure 4. A declined trend was observed in the effluent water quality in the PAP system as the duration of rainfall was prolonged. The effluent water quality order with the whole rainfall event processing was MZP-PM > zeolite bedding > limestone bedding. The results showed that the collective removal of nutrients by zeolite (33.7–62.7%) was slightly higher than that of limestone (26.3–56.4%) (Figure 4) whilst the heights of zeolite applied in the PAP system were the same. The amounts of nutrients removed by the limestone PAP system were much lower. It may be due to the higher adsorption potential of the zeolite of the Langmuir model (Table 1). On the other hand, the removal was insufficient because the high concentrations of nutrients in the effluent would adversely affect the aquatic

organisms and plants in the urban rivers [30]. The post treating with a horizontal filter column packed with MZP-PM gave greater removal of nutrients (82.2% NH_4^+-N and 81.9% TP). An additional amount of nutrients was removed by MZP-PM, equivalent to 4.2% of the volume of zeolite and limestone, which was considerable. It is due to the extremely elevated adsorption ability of MZP-PM (Langmuir adsorption capacities of 9.72 and 1.23 mg/g for NH_4^+-N and TP (Table 1) compared with zeolite and limestone in the range of 1.31–3.34 mg/g for NH_4^+-N and 0.42–0.55 mg/g for TP). The adsorption capacity of MZP-PM was 3–8 times greater than that of zeolite and 2–3 times greater than that of limestone. Batch adsorption data in Table 1 showed that MZP-PM had a higher adsorption capacity to NH_4^+-N than that of TP. It had been reported that modified zeolite adsorbents exhibited higher adsorption capacity [19,26]. However, in the PAP system, the mixture of nutrients with MZP-PM had a higher adsorption capacity for TP because of the lower influent concentration of TP (1.2 mg/L) than NH_4^+-N (5.2 mg/L). Nevertheless, both the NH_4^+-N and TP were almost completely removed by MZP-PM in the initial stages of the rainfall event (Table 2).

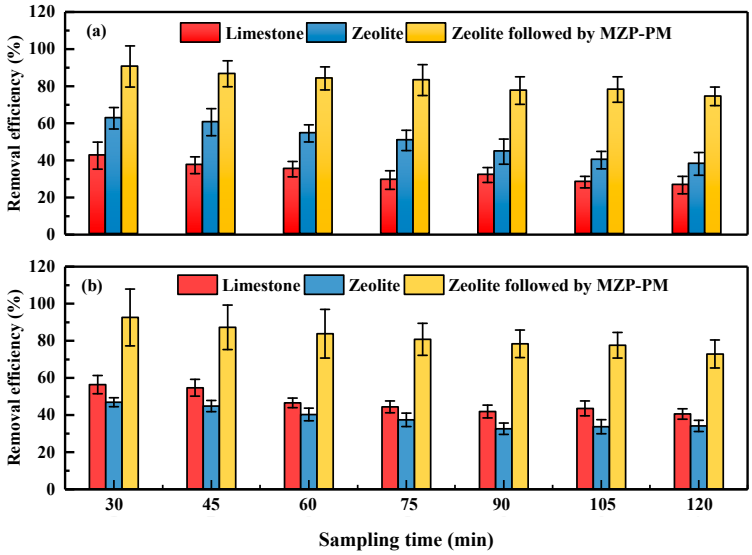

Figure 4. Removal efficiency of NH_4^+-N (**a**) and TP (**b**) in limestone, zeolite bedding and zeolite followed by MZP-PM during a typical rainfall.

Table 2. Cumulative adsorption of nutrients (q_{total}).

PAP System Materials	Units	NH_4^+-N	TP
Influent concentration	mg/L	5.2	1.2
Total added	mg	39	9
Limestone bed, q_{total}	mg	12.91	4.22
Zeolite bed, q_{total}	mg	20.28	3.47
Zeolite bed followed by MZP-PM, q_{total}	mg	32.01	7.37
Limestone bed [a]	%	33.1	46.9
Zeolite bed [a]	%	50.2	38.5
Zeolite bed followed by MZP-PM [a]	%	82.2	81.9

[a] Percentage of cumulative nutrients adsorption = (cumulative nutrients added—cumulative nutrients in effluent)/cumulative nutrients added.

The removal efficiency of MZP-PM to NH_4^+-N and TP decreased from 90.6% to 74.5% and from 92.6% to 72.9% as the duration of the rainfall event (Figure 4). This result was because of a permanent number of adsorption sites on the MZP-PM surface for a fixed dose. As the rainfall event was enhanced, the adsorption among nutrients would decrease so that the adsorption efficiency becomes reduced. At the initial rainfall event, all the available sites

of adsorption on MZP-PM were accessible and involved in removing nutrients so that the overall adsorption was more efficient. While for the fixed MZP-PM dose, as the cumulative contents of N and P enhanced, the utilization of accessible adsorption sites enhanced and as a result, the removal efficiency was reduced [26,31]. Due to the differences in the features of water quality and quantity of rainfall in different regions, and the adsorption of N and P by MZP-PM would gradually become saturated. Therefore, it is necessary to discuss the replacement cycle of the filter column. The tests were performed with continuous rain at an intensity of 82.31 mm h^{-1} for 2 h, which is equivalent to 59.76 mm of total rainfall that on mean value occurred in Nanjing. According to Maryam's reports [32] and the adsorption characteristics of MZP-PM in this study (Equation (6)), the approximate replacement period of the medium is about 15 months.

$$S = \frac{Q_e \times 1000}{\overline{R} \times D/q \times 1100} \tag{6}$$

where S is the replacement cycle of the filter column, Q_e is the adsorption capacities of MZP-PM, $\overline{R}$ is the average removal concentrations, D is the water volume, q is the average intensity of this rainfall and the average annual rainfall in Nanjing is about 1100 mm $year^{-1}$.

3.3. Water Quantity Assessment

The environmental quality standards for surface water trigger values in China were employed to evaluate whether the concentration of nutrients in the effluent of the PAP system was safe to the natural water bodies [33]. The results revealed that the PAP system with zeolite and limestone bedding layers was unable to reduce the nutrient concentrations below the trigger values for class IV standard for surface water.

The variations of Nemerow index at various sampling times of three sets of experiments are shown in Figure 5. The nutrients' concentrations slowly increased until about 90 min while the concentrations in effluent remained constant were between 3.1–3.8 mg/L for NH_4^+-N, 0.7–0.8 mg/L for TP in limestone and zeolite bedding, respectively. By the end of the artificial rainfall event, from 90 to 120 min, the Nemerow indices in both PAP systems with limestone and zeolite bedding were approximately close to 1.8. As a result, they all exceeded the standard water quality of Class V for surface water in China. In comparison, the Nemerow index of the PAP system with zeolite followed by MZP-PM increased slowly within the first 60 min, which remained below 0.8 upon the whole rainfall event, demonstrating that the initial effluent was even capable of meeting water quality standards of class II for surface water. The effluent gradually dropped to the class IV of water quality standards in 90 min, even after the end of the rainfall event, but it could still reach the class V for surface water as the rainfall event continued, which was much more efficient than the PAP system with limestone and zeolite. The results showed that the discharge of stormwater from the tested PAP system with MZP-PM as a post-treatment was appropriate for draining into surface water.

The PAP system with an MZP-PM column was designed to process stormwater runoff comparatively at low rainfall intensity, which could enhance the nutrients removal. This enables the PAP system as a perfect low impact developed selection to process small stormwater events. Although enhanced adsorbent is important for the removal of nutrients, MZP-PM (modified zeolite porous microspheres) did not significantly influence NO_3^--N and NO_2^--N removal in the presented research. Hence, more research is required in this field, including removal of heavy metals and total nitrogen, analysis period of adsorption, and minimum pore water contact time in the MZP-PM needed for a target N and P elimination objective.

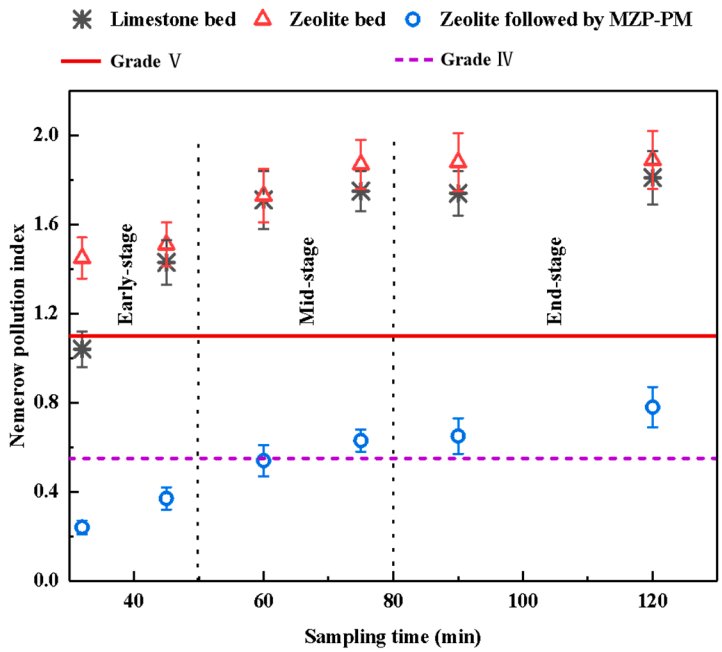

Figure 5. Results of Nemerow index in the artificial rainfall event.

3.4. Ammonium and Phosphate Adhesion onto Loaded MZP-PM

3.4.1. Ammonium Adhesion onto Loaded MZP-PM

The mechanism of ion-exchange for removing the ammonium by MZP-PM could be achieved by calculating the metal ion concentration in the adsorbing solution of ammonium onto MZP-PM [34]. The AAS assessment confirmed that the release of Na^+ with a minor metal ion including K^+, Mg^{2+}, and Ca^{2+} during the process of ammonium adsorption. The equilibrium adsorption of ammonium was 7.94 mg/g shown in Table 3. The concentration of K^+, Mg^{2+}, and Ca^{2+} equaled the ion exchange contents NH_4^+-N (IE-N 6.17 mg) 77.8 ± 2.52%. As a result, the physisorption of NH_4^+-N (PA-N 1.77 mg/L) was 22.2 ± 1.76%.

Table 3. Adhesion of ammonium and phosphate adsorbed onto MZP-PM (25 °C, pH = 7, initial concentration of N = 20 mg/L, P = 5 mg/L, time = 24 h).

Q_e (N)		IE-N			PA-N	
mg/g		mg/g	%		mg/g	%
7.94		6.17 ± 0.21	77.8 ± 2.52		1.77 ± 0.14	22.2 ± 1.76
Q_e (P)	La-P		LB-P		R-P	
mg/g	mg/g	%	mg/g	%	mg/g	
2.07	1.33 ± 0.08	64.3 ± 3.86	0.43 ± 0.11	20.78 ± 5.31	0.31 ± 0.06	14.92 ± 2.89

3.4.2. Phosphate Speciation onto Loaded MZP-PM

The finding of phosphate speciation by MZP-PM are given in Table 3. The results demonstrate that a considerable part of phosphate is retained onto MZP-PM because of the incorporation of La^{3+} (La-P) with 64.3 ± 3.86%. Therefore, it indicated that the La-OH groups of MZP-PM were mainly responsible for the adsorption of phosphate. The 20.78 ± 5.31% of loosely bounded phosphate fraction (LB-P) immobilized was related and the 14.92 ± 2.89 of residual phosphate (R-P) was lower, illustrating that the process of removal of phosphate by MZP-PM was not irreversible, which would have an important in the removal of phosphate application. Hence, it was concluded that the mechanisms of phosphate adsorption on MZP-PM mainly lie on ligand exchange and electrostatic interaction. The proposed adsorption mechanisms of NH_4^+-N and TP onto MZP-PM are given in Figure 6.

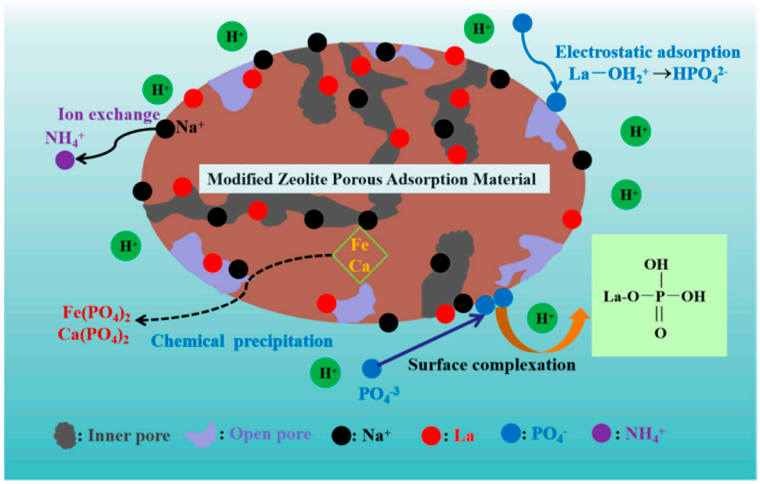

Figure 6. The suggested adsorption mechanism of ammonium and phosphate simultaneously onto MZP-PM.

3.5. Adsorption Mechanism

3.5.1. SEM-EDS Study

The morphology of MZP-PM before and after the adsorption during experiments is presented in Figure 7. The SEM images indicate that NH_4^+-N and TP were adsorbed onto MZP-PM, leading to the distribution of spherical particles onto the surface, and the protuberances formation (a stacking structure) reduced the intra-particle void size. The morphology of MZP-PM become changed after the adsorption of phosphate into crystallization onto the active sites, which increased the particle size. EDS analysis confirmed the existence of O, Ca, La, Na, Al, and Si as the major elements in the composition of MZP-PM, indicating the possible formation of the La-P complex. The given observations were in accordance with the results of phosphate speciation onto loaded MZP-PM. From another point of view, the weight of Na^+ decreased from 9.5% to 4.5% upon the adsorption of NH_4^+-N and TP. Thus, this phenomenon decreased the Na^+ and the existence of N in the EDS image demonstrated the exchange of Na^+ with NH_4^+-N.

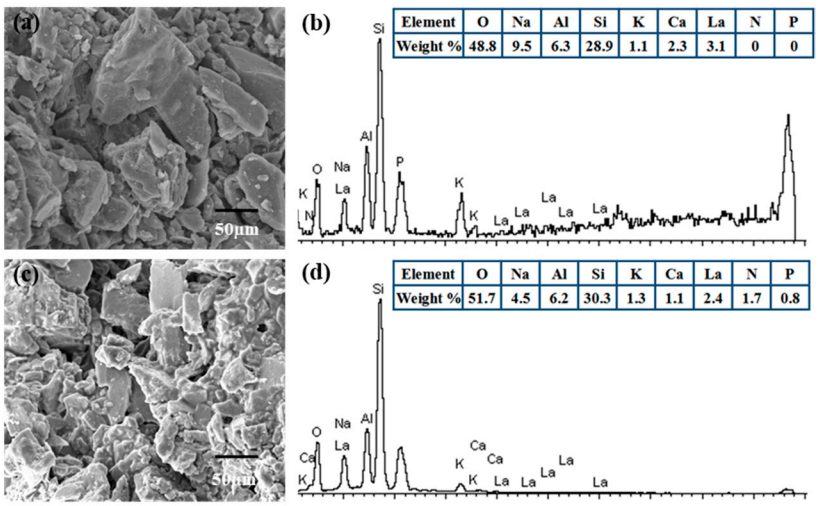

Figure 7. Scanning electron microscopy (SEM) images and corresponding EDS data of MAP-PAM before adsorption (**a**,**b**) and after adsorption (**c**,**d**).

3.5.2. FTIR Study

The FTIR spectrum of MZP-PM before and after the adsorption of NH_4^+-N and TP are shown in Figure 8. The typical broad peaks at 3429 cm^{-1} and 1625 cm^{-1} corresponded

to the hydroxyl group blending and stretching vibration of adsorbed water [35], respectively. The MZP-PM showed several new adsorption peaks at 1401 cm^{-1} and 1076 cm^{-1} upon adsorption compared with the original one, which was associated with the N-H symmetric bending vibrations, the change in the intensity of the two absorption peaks may be caused by the hydrolysis of La_2O_3 on the surface of the zeolite to form La-OH hydroxyl group. This result indicates that the elimination of NH_4^+-N onto the MZP-PM was majorly done through chemisorptions. The occurrence of NH_4^+-N was ascribed to the Na^+ ion exchangeability in MZP-PM with NH_4^+ in the solution. A small broad and weak band at 1076 cm^{-1} presumably resulted from the characteristic of the asymmetric stretch vibration of P-O. Thus, it was concluded that the hydroxyl group of MZP-PM can be replaced through ligand exchange by the adsorbed phosphate. The results were in good agreement with previous studies, showing that at neutral pH the ligand-exchange processing resulted in the development of protonated mono and bi dentate species on lanthanum oxide surfaces [19,36].

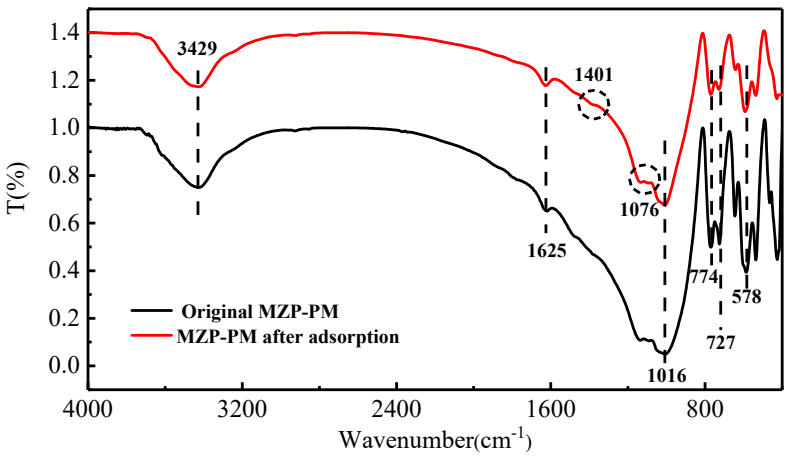

Figure 8. FTIR spectra of MZP-PM before and after reaction with NH_4^+-N and TP.

3.5.3. XPS Study

The XPS spectra of MZP-PM before and after the NH_4^+-N and TP adsorption at pH 7.0 were investigated. The XPS full-range spectra of MZP-PM before and after the adsorption are given in Figure 9. The presence of a distinct centered peak at 835.8 eV indicated the intercalation of La-oxides onto the zeolite powder. Relatively, a distinct P 2p binding energy peak at 131.7 eV after the adsorption of phosphate onto MZP-PM, demonstrating the feasible adsorption. The standard P 2p spectrum originated from KH_2PO_4 purified sample, is appeared at 134.0 eV and the obvious shifts of 0.5 eV to lower energy level demonstrated the strong affinities between phosphate and MZP-PM. As shown in Figure 9b, c, the representative satellite peaks of La $3d_{5/2}$ for original MZP-PM were located at 834.9 eV and 838.3 eV, respectively. The phosphate adsorption led to the apparent transformation of the proportion onto La $3d_{5/2}$ double peaks and a visible peak shift to higher binding energy, indicating the new La-complex formation [37]. The large shifts of 0.6 and 1.1 eV indicated the existence of strong affinities by metal oxide surface through the formations of potentially mono and bi dentate inner-sphere surface complexes [38]. The atomic fraction of Na (1070.12 eV) decreased from 9.5% to 4.5% upon adsorption, implying that NH_4^+-N was most probably eliminated by ion-exchange with Na^+, which was in accordance with the results of the ammonium speciation experiment.

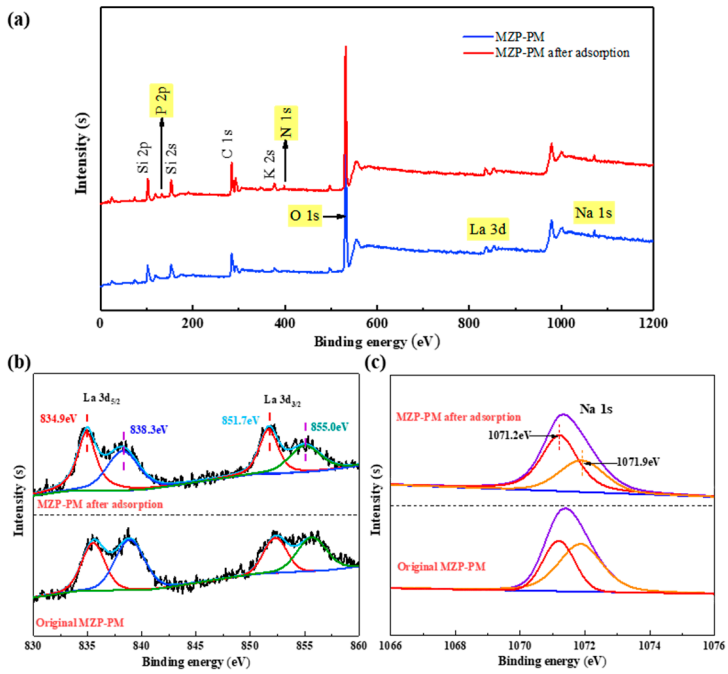

Figure 9. XPS analysis of MZP-PM before or after adsorption. (**a**) XPS survey scan of MZP-PM before and after adsorption; (**b**) La 3d5/2 spectra and (**c**) Na 1s spectra before and after adsorption.

The concentration of NH_4^+-N and TP in the current study were investigated by the single factor experiment approach. Usually, numerous factors could influence the elimination efficiency of the PAP system simultaneously with an MZP-PM filter column in practical road projects. For instance, adsorption and removal efficiencies are affected by rainfall intensity, temperature, and pollution levels in different seasons. Therefore, in terms of practical application, further research about the effect of weather conditions, the conformation of stormwater, and loading levels on the elimination of other contaminants such as TSS, COD, and heavy metals are recommended.

4. Conclusions

In this work, NaOH-activated with $LaCl_3$-impregnated synthetic modified zeolite porous microspheres (MZP-PM) were designed, aiming at increasing N and P retention efficiency by exchanging with sodium for NH_4^+-N and surface complexion for TP. Two laboratory-scale PAP systems were developed by comparing limestone bedding and zeolite incorporated into MZP-PM as a filter column under a typical rainfall. The following conclusions were made by the experimental results.

(1) Batch adsorption data from solutions of nutrients mixtures onto the two PAP system bedding layers and the MZP-PM fitted the Langmuir model with adsorption capacities in the following order: MZP-PM > zeolite > limestone for NH_4^+-N and MZP-PM > limestone > zeolite for TP.

(2) Augmentation of ammonium and phosphate elimination from stormwater runoff was effectively achieved in the PAP system with an MZP-PM column of adsorbent as a post-treatment. During the rainfall events, the study demonstrated by the zeolite or limestone-based PAP system didn't remove NH_4^+-N and TP in stormwater that passed through this system completely and the concentrations of nutrients in effluent couldn't meet the standard quality of surface water. While a post-treatment with a filter column containing MZP-PM (<5% of zeolite weight) was added to the zeolite-based PAP system, 72.9–92.6% of the nutrients were eliminated. The combined treatment was satisfactory and effluent met the standards criteria of surface water.

(3) Speciation pathway and XPS, FTIR analysis established that ammonium removal was mainly ascribed to exchanging with sodium in the adsorbent, and phosphate adsorp-

tion mainly followed the surface complexion mechanism, the surface hydroxyl groups played the key role.

Author Contributions: Conceptualization, H.L. and Z.J.; methodology, H.L.; software, B.H.; validation, W.Z.; formal analysis, W.Z.; investigation, H.L.; resources, Z.J.; data curation, W.Z.; writing—original draft preparation, H.L.; writing—review and editing, Z.J.; visualization, B.H. and W.Z.; supervision, Z.J.; project administration, Z.J.; funding acquisition, Z.J. All authors have read and agreed to the published version of the manuscript.

Funding: This research was funded by the National Science and Technology Support Program (2015BAL02B04); the Technology Project of China Housing and Urban Rural Development Ministry (2015-K7-012); a Project Funded by the National First-class Disciplines (PNFD), and a Project Funded by the Priority Academic Program Development of Jiangsu Higher Education Institutions (PAPD).

Institutional Review Board Statement: Not applicable.

Informed Consent Statement: Not applicable.

Data Availability Statement: The datasets used during the current study are available from the corresponding author on reasonable request.

Acknowledgments: The authors would like to thank Zeyu Zhang and Simin Zuo for their assitance in the laboratory experiment.

Conflicts of Interest: The authors declare no conflict of interest. The funders had no role in the design of the study; in the collection, analyses, or interpretation of data; in the writing of the manuscript, or in the decision to publish the results.

References

1. de Macedo, M.B.; do Lago, C.A.F.; Mendiondo, E.M. Stormwater volume reduction and water quality improvement by bioretention: Potentials and challenges for water security in a subtropical catchment. *Sci. Total Environ.* **2019**, *647*, 923–931. [CrossRef]
2. Lintern, A.M.; DeLetic, A.; Leahy, P.J.; McCArthy, D.T. Digging up the dirty past: Evidence for stormwater's contribution to pollution of an urban floodplain lake. *Mar. Freshw. Res.* **2015**, *66*, 596–608. [CrossRef]
3. Jiang, W.; Sha, A.; Xiao, J.; Li, Y.; Huang, Y. Experimental study on filtration effect and mechanism of pavement runoff in permeable asphalt pavement. *Constr. Build. Mater.* **2015**, *100*, 102–110. [CrossRef]
4. Kumar, K.; Kozak, J.; Hundal, L.; Cox, A.; Zhang, H.; Granato, T. In-situ infiltration performance of different permeable pavements in a employee used parking lot—A four-year study. *J. Environ. Manag.* **2016**, *167*, 8–14. [CrossRef]
5. Tippler, C.; Wright, I.A.; Davies, P.J.; Hanlon, A. The influence of concrete on the geochemical qualities of urban streams. *Mar. Freshw. Res.* **2014**, *65*, 1009. [CrossRef]
6. Braswell, A.S.; Winston, R.J.; Hunt, W.F. Hydrologic and water quality performance of permeable pavement with internal water storage over a clay soil in Durham, North Carolina. *J. Environ. Manag.* **2018**, *224*, 277–287. [CrossRef] [PubMed]
7. Razzaghmanesh, M.; Borst, M. Long-term effects of three types of permeable pavements on nutrient infiltrate concentrations. *Sci. Total Environ.* **2019**, *670*, 893–901. [CrossRef] [PubMed]
8. He, B.J.; Zhu, J.; Zhao, D.X.; Gou, Z.H.; Qi, J.D.; Wang, J. Co-benefits approach: Opportunities for implementing sponge city and urban heat island mitigation. *Land Use Policy* **2019**, *86*, 147–157. [CrossRef]
9. Wright, I.A.; Davies, P.J.; Findlay, S.J.; Jonasson, F.O.J. A new type of water pollution: Concrete drainage infrastructure and geochemical contamination of urban waters. *Mar. Freshw. Res.* **2011**, *62*, 1355–1361. [CrossRef]
10. Collins, K.; Hunt, W.; Hathaway, J. Side-by-Side Comparison of Nitrogen Species Removal for Four Types of Permeable Pavement and Standard Asphalt in Eastern North Carolina. *J. Hydrol. Eng.* **2010**, *15*, 512–521. [CrossRef]
11. Drake, J.; Bradford, A.; Van Seters, T. Stormwater quality of spring–summer-fall effluent from three partial-infiltration permeable pavement systems and conventional asphalt pavement. *J. Environ. Manag.* **2014**, *139*, 69–79. [CrossRef] [PubMed]
12. Luo, H.; Guan, L.; Jing, Z.; Zhang, Z.; Wang, Y. Influence of filter layer positions and hydraulic retention time on removal of nitrogen and phosphorus by porous asphalt pavement. *Water Sci. Technol.* **2020**, *81*, 445–455. [CrossRef] [PubMed]
13. Ostrom, T.K.; Davis, A.P. Evaluation of an enhanced treatment media and permeable pavement base to remove stormwater nitrogen, phosphorus, and metals under simulated rainfall. *Water Res.* **2019**, *166*, 115071.1–115071.12. [CrossRef]
14. Kuruppu, U.; Rahman, A.; Sathasivan, A. Enhanced denitrification by design modifications to the standard permeable pavement structure. *J. Clean. Prod.* **2019**, *237*, 117721. [CrossRef]
15. Davis, A.; Liu, J. Phosphorus Speciation and Treatment Using Enhanced Phosphorus Removal Bioretention. *Environ. Sci. Technol.* **2013**, *48*, 607–614.
16. He, Y.; Lin, H.; Dong, Y.; Wang, L. Preferable adsorption of phosphate using lanthanum-incorporated porous zeolite: Characteristics and mechanism. *Appl. Surf. Sci.* **2017**, *426*, 995–1004. [CrossRef]
17. Shen, D.; Li, T.; Shen, F.; Wang, Z. Phosphate adsorption on lanthanum loaded biochar. *Chemosphere* **2016**, *150*, 1–7.

18. Zhao, Y.; Zhou, S.; Zhao, C.; Valeo, C.J.W. The Influence of Geotextile Type and Position in a Porous Asphalt Pavement System on Pb (II) Removal from Stormwater. *Nansosale* **2018**, *10*, 1205. [CrossRef]
19. He, Y.; Lin, H.; Dong, Y.; Liu, Q.; Wang, L.J.C. Simultaneous removal of ammonium and phosphate by alkaline-activated and lanthanum-impregnated zeolite. *Chemosphere* **2016**, *164*, 387–395. [CrossRef]
20. Yang, J.; Yuan, P.; Chen, H.Y.; Zou, J.; Yuan, Z.; Yu, C. Rationally designed functional macroporous materials as new adsorbents for efficient phosphorus removal. *J. Mater. Chem.* **2012**, *22*, 9983–9990. [CrossRef]
21. Ergas, S.J.; Sengupta, S.; Siegel, R.; Pandit, A.; Yao, Y.; Yuan, X. Performance of Nitrogen-Removing Bioretention Systems for Control of Agricultural Runoff. *J. Environ. Manag.* **2010**, *136*, 1105–1112. [CrossRef]
22. Lucke, T.; Nichols, P.W.B. The pollution removal and stormwater reduction performance of street-side bioretention basins after ten years in operation. *Sci. Total Environ.* **2015**, *536*, 784–792. [CrossRef] [PubMed]
23. Silveira, A.J.R. Cumulative equations for continuous time Chicago hyetograph method. *RBRH* **2016**, *21*, 646–651. [CrossRef]
24. Jiang, C.; Li, J.; Li, H.; Li, Y. Nitrogen retention and purification efficiency from rainfall runoff via retrofitted bioretention cells. *Sep. Purif. Technol.* **2019**, *220*, 25–32. [CrossRef]
25. Mazurek, R.; Kowalska, J.; Gsiorek, M.; Zadrony, P.; Orowska, K.J.C. Assessment of heavy metals contamination in surface layers of Roztocze National Park forest soils (SE Poland) by indices of pollution. *Chemosphere* **2017**, *168*, 839–850. [CrossRef]
26. Xu, Q.; Li, W.; Ma, L.; Cao, D.; Owens, G.; Chen, Z. Simultaneous removal of ammonia and phosphate using green synthesized iron oxide nanoparticles dispersed onto zeolite. *Sci. Total Environ.* **2019**, *703*, 135002. [CrossRef]
27. Huo, H.; Hai, L.; Dong, Y.; Huang, C.; Han, W.; Cao, L. Ammonia-nitrogen and phosphates sorption from simulated reclaimed waters by modified clinoptilolite. *J. Hazard. Mater.* **2012**, *229–230*, 292–297. [CrossRef]
28. Chen, Y. Study on Ammonia Nitrogen Removal from Simulated Wastewater by Macroporous Sintered Zeolite Ball. Master's Thesis, Hangzhou Normal University, Hangzhou, China, 2018.
29. Kuroki, V.; Bosco, G.E.; Fadini, P.S.; Mozeto, A.A.; Cestari, A.R.; Carvalho, W. Use of a La(III)-modified bentonite for effective phosphate removal from aqueous media. *J. Hazard. Mater.* **2014**, *274*, 124–131. [CrossRef]
30. Gao, Y.; Jia, Y.; Yu, G.; He, N.; Zhang, L.; Wang, Y. Anthropogenic reactive nitrogen deposition and associated nutrient limitation effect on gross primary productivity in inland water of China. *J. Clean. Prod.* **2018**, 208. [CrossRef]
31. Wan, C.; Ding, S.; Zhang, C.; Tan, X.; Zou, W.; Liu, X.; Yang, X.J.S.; Technology, P. Simultaneous recovery of nitrogen and phosphorus from sludge fermentation liquid by zeolite adsorption: Mechanism and application. *Sep. Purif. Technol.* **2017**, *180*, 1–12. [CrossRef]
32. Ghavanloughajar, M.; Valença, R.; Le, H.; Rahman, M.; Borthakur, A.; Ravi, S.; Stenstrom, M.; Mohanty, S. Compaction conditions affect the capacity of biochar-amended sand filters to treat road runoff. *Sci. Total Environ.* **2020**, *735*, 139180. [CrossRef] [PubMed]
33. Ministry of Ecology and Environment. *Environmental Quality Standards for Surface Water*; Chinese Environmental Science Press: Beijing, China, 2002.
34. Malekian, R.; Eslamian, S.; Mousavi, S.-F.; Mikayilov, F.; Majid, A. Ion-exchange process for ammonium removal and release using natural Iranian zeolite. *Appl. Clay Sci.* **2011**, *51*, 323–329. [CrossRef]
35. Wahab, M.; Jellali, S.; Jedidi, N. Ammonium biosorption onto sawdust: FTIR analysis, kinetics and adsorption isotherms modeling. *Bioresour. Technol.* **2010**, *101*, 5070–5075. [CrossRef]
36. Makita, Y.; Sonoda, A.; Sugiura, Y.; Ogata, A.; Separation, K.O.J.; Technology, P. Phosphorus Removal from Model Wastewater Using Lanthanum Hydroxide Microcapsules with Poly(Vinyl Chloride) Shells. *Sep. Purif. Technol.* **2020**, *241*, 116707. [CrossRef]
37. Zhang, C.; Li, Y.; Wang, F.; Yu, Z.; Wei, J.; Yang, Z.; Ma, C.; Li, Z.; Xu, Z.Y.; Zeng, G. Performance of magnetic zirconium-iron oxide nanoparticle in the removal of phosphate from aqueous solution. *Chemosphere* **2017**, *396*, 1783–1792. [CrossRef]
38. Zhang, Q.; Teng, J.; Zou, G.; Peng, Q.; Du, Q.; Jiao, T.; Xiang, J. Efficient phosphate sequestration for water purification by unique sandwich-like MXene/magnetic iron oxide nanocomposites. *Nanoscale* **2016**, *8*, 7085–7093. [CrossRef]